Design and MHD Diagnostics of a STAR-like Spherical Tokamak Equilibrium with `FreeGSNKE`

Juan Pablo Solís Ruiz

December 7, 2025

Abstract

This work presents the design, construction and analysis of a spherical tokamak equilibrium, inspired by the reactor–scale STAR concept, using the `FreeGSNKE` Grad–Shafranov solver.

Starting from a simple Miller–type target plasma boundary (major radius, aspect ratio, elongation and triangularity), a completely new "STAR-like" machine is built: inner and outer walls, a set of poloidal field (PF) coils, a central solenoid (CS), and a shaped target plasma boundary.

On top of this machine, axisymmetric MHD equilibria are computed by solving the Grad–Shafranov equation with self–consistent pressure and toroidal current profiles generated by the `ConstrainPaxisIp` module. A systematic scan of PF/CS currents, followed by a local micro–scan, is used to shape the plasma. The first iteration yields an almost circular equilibrium, while the refined configuration is a strongly triangular (*bean-shaped*) spherical tokamak equilibrium with low aspect ratio, high elongation and positive triangularity.

For this bean–shaped STAR-like equilibrium, several diagnostics are computed: separatrix geometry, safety factor profile $q(\psi)$, pressure profile and poloidal beta, toroidal current density $j_\phi(R, Z)$, approximate magnetic shear $\hat{s}(\psi)$ and net forces on the coils. The physical interpretation of these results is discussed in the context of STAR-like spherical tokamak design.

Contents

1 Physical framework: axisymmetric MHD equilibrium

1.1 Static MHD equilibrium and toroidal symmetry

We consider a static, single–fluid MHD equilibrium governed by

$$\nabla p = \mathbf{j} \times \mathbf{B}, \tag{1}$$
$$\nabla \times \mathbf{B} = \mu_0 \mathbf{j}, \tag{2}$$
$$\nabla \cdot \mathbf{B} = 0, \tag{3}$$

where p is the scalar pressure, $\mathbf{B}$ the magnetic field, $\mathbf{j}$ the current density and μ_0 the vacuum permeability.

In an axisymmetric tokamak, it is natural to use cylindrical coordinates (R, ϕ, Z), with ϕ the toroidal angle and $\partial/\partial\phi = 0$. Under this symmetry, the magnetic field can be written in terms of a poloidal flux function $\psi(R, Z)$ and a toroidal field function $F(\psi)$:

$$\mathbf{B} = \frac{1}{R}\nabla\psi(R, Z) \times \hat{\boldsymbol{\phi}} + \frac{F(\psi)}{R}\,\hat{\boldsymbol{\phi}}, \tag{4}$$

where ψ is proportional to the poloidal magnetic flux enclosed by a toroidal ring of radius R.

Combining (1) with $\partial/\partial\phi = 0$ implies that both the pressure and F depend only on ψ:

$$p = p(\psi), \qquad F = F(\psi). \tag{5}$$

These two functions encode the radial structure of pressure and toroidal field in the plasma.

1.2 Grad–Shafranov equation

Substituting (4) into Ampère's law and (1) yields the Grad–Shafranov equation for the poloidal flux $\psi(R, Z)$:

$$\Delta^*\psi = -\mu_0 R^2 \frac{\mathrm{d}p(\psi)}{\mathrm{d}\psi} - \frac{1}{2}\frac{\mathrm{d}F^2(\psi)}{\mathrm{d}\psi}, \tag{6}$$

where the so–called Grad–Shafranov operator Δ^* is

$$\Delta^*\psi = R\frac{\partial}{\partial R}\left(\frac{1}{R}\frac{\partial\psi}{\partial R}\right) + \frac{\partial^2\psi}{\partial Z^2}. \tag{7}$$

Equation (6) is nonlinear through the dependence of the right–hand side on ψ via $p(\psi)$ and $F(\psi)$.

Given:

- a vacuum vessel and conductor geometry defining the computational domain and boundary conditions for ψ,
- profiles $p(\psi)$ and $F(\psi)$,

the Grad–Shafranov problem consists in finding $\psi(R, Z)$ satisfying (6) with appropriate conditions on the wall(s). This is exactly what `FreeGSNKE` solves numerically.

1.3 Derived quantities: $q(\psi)$, β and currents

Once $\psi(R, Z)$ is known, several key MHD quantities can be obtained:

- The toroidal current density j_ϕ follows from

$$\mu_0 j_\phi = \frac{1}{R}\Delta^*\psi,$$

  or, in practice, from the discrete Grad–Shafranov operator acting on the numerical solution ψ_{ij}.

- The safety factor $q(\psi)$ is, in flux coordinates,

$$q(\psi) = \frac{1}{2\pi}\oint \frac{\mathbf{B}\cdot\nabla\phi}{\mathbf{B}\cdot\nabla\theta}\,\mathrm{d}\theta,$$

  where θ is a poloidal angle. In `FreeGSNKE`, $q(\psi)$ is computed by an internal integral routine that we access through `eq.q(psinorm)`.

- The volume–averaged toroidal beta is

$$\beta_T = \frac{2\mu_0\langle p\rangle}{B_0^2},$$

  where $\langle p\rangle$ is the volume average of p inside the separatrix and B_0 is a characteristic toroidal field at the plasma major radius (in our case, approximated by $B_0 \simeq f_{\mathrm{vac}}/R_0^{\mathrm{plasma}}$).

- The poloidal beta β_p can be defined in several ways; here we use the definition implemented in `eq.poloidalBeta1()`, which involves volume integrals of pressure and poloidal magnetic field.

These diagnostics are used extensively in the bean–shaped STAR–like equilibrium discussed later.

2 Numerical framework: `FreeGSNKE` and solution strategy

2.1 Rectangular grid and discrete Grad–Shafranov operator

All equilibria are computed on a uniform rectangular grid (R_i, Z_j) that covers a domain slightly larger than the outer wall. Let $(R_{\mathrm{outer}}(\theta), Z_{\mathrm{outer}}(\theta))$ be the outer vessel contour produced by the geometry routine. The numerical domain bounds are chosen as

$$R_{\min} = \min_\theta R_{\mathrm{outer}}(\theta) - \Delta_R^{\mathrm{margin}}, \tag{8}$$

$$R_{\max} = \max_\theta R_{\mathrm{outer}}(\theta) + \Delta_R^{\mathrm{margin}}, \tag{9}$$

$$Z_{\min} = \min_\theta Z_{\mathrm{outer}}(\theta) - \Delta_Z^{\mathrm{margin}}, \tag{10}$$

$$Z_{\max} = \max_\theta Z_{\mathrm{outer}}(\theta) + \Delta_Z^{\mathrm{margin}}. \tag{11}$$

Typical grid sizes used here are in the range

$$(n_R, n_Z) \sim (65, 129)$$

for coarse scans, and up to

$$(n_R, n_Z) \sim (129, 257)$$

for high–resolution diagnostics.

On this grid, the Grad–Shafranov operator Δ^* is discretised with second–order finite differences, yielding a linear operator $\mathcal{L}[\psi_{ij}]$ that approximates $\Delta^*\psi$ at each grid point.

2.2 Profiles $p(\psi)$ and $F(\psi)$ via `ConstrainPaxisIp`

The class `ConstrainPaxisIp` is used to build smooth pressure and toroidal field profiles starting from a small set of global parameters:

- on–axis pressure p_{axis},
- total plasma current I_p,
- vacuum parameter f_{vac} (setting B_ϕ in the vacuum),
- shape exponents (α_m, α_n).

Using the normalised poloidal flux

$$\bar{\psi} = \frac{\psi - \psi_{\text{axis}}}{\psi_{\text{sep}} - \psi_{\text{axis}}}, \qquad \bar{\psi} \in [0, 1],$$

`ConstrainPaxisIp` builds profiles of the form

$$p(\bar{\psi}) \propto p_{\text{axis}}(1 - \bar{\psi})^{\alpha_m + 1}, \tag{12}$$

$$F^2(\bar{\psi}) \simeq f_{\text{vac}}^2 + \Delta F^2 (1 - \bar{\psi})^{\alpha_n + 1}, \tag{13}$$

and adjusts ΔF^2 so that the toroidal current density integrated over the plasma volume reproduces the desired I_p. Throughout this work we use typical values

$$\alpha_m \approx 1.8, \qquad \alpha_n \approx 1.2,$$

producing reasonably smooth pressure and current profiles.

2.3 Newton–Krylov solver: `GSstaticsolver.NKGSsolver`

The discretised Grad–Shafranov equation can be written as a nonlinear system for the vector of nodal fluxes $\boldsymbol{\psi}$:

$$\mathbf{F}(\boldsymbol{\psi}) = \mathbf{0},$$

where $\mathbf{F}$ denotes the residual of (6) together with boundary conditions on the wall.

`FreeGSNKE` provides the class `GSstaticsolver.NKGSsolver`, which implements a Newton–Krylov algorithm:

1. Start from an initial guess $\boldsymbol{\psi}^{(0)}$, typically the solution from a previous nearby equilibrium or a simple smooth profile.
2. At iteration k, compute the residual $\mathbf{r}^{(k)} = \mathbf{F}(\boldsymbol{\psi}^{(k)})$.
3. Linearise:

   $$\mathbf{J}^{(k)} \delta\boldsymbol{\psi}^{(k)} = -\mathbf{r}^{(k)},$$

   where $\mathbf{J}^{(k)}$ is the Jacobian of $\mathbf{F}$.

4. Solve the linear system using a Krylov method (e.g. GMRES) with suitable preconditioning, as provided by `SciPy`.

5. Update
$$\boldsymbol{\psi}^{(k+1)} = \boldsymbol{\psi}^{(k)} + \delta\boldsymbol{\psi}^{(k)}.$$

6. Iterate until the relative residual norm falls below a prescribed tolerance (typically 10^{-8} for high–accuracy runs).

In the STAR–like bean–shaped cases, convergence with final relative residuals $\sim 10^{-9}$ is obtained in $\mathcal{O}(20\text{–}30)$ Newton iterations.

3 Machine geometry and PF/CS system

3.1 Target Miller boundary

The target plasma boundary is specified using a standard Miller parametrisation that is up–down symmetric:

$$R_p(\theta) = R_0^{(\mathrm{geom})} + a^{(\mathrm{geom})} \cos\bigl(\theta + \delta^{(\mathrm{geom})} \sin\theta\bigr), \tag{14}$$
$$Z_p(\theta) = \kappa^{(\mathrm{geom})} a^{(\mathrm{geom})} \sin\theta, \tag{15}$$

with $\theta \in [0, 2\pi]$. The geometric target parameters are chosen as

$$R_0^{(\mathrm{geom})} \approx 4.0\,\mathrm{m}, \tag{16}$$
$$A^{(\mathrm{geom})} \approx 1.7, \qquad a^{(\mathrm{geom})} = \frac{R_0^{(\mathrm{geom})}}{A^{(\mathrm{geom})}} \approx 2.35\,\mathrm{m}, \tag{17}$$
$$\kappa^{(\mathrm{geom})} \approx 1.8, \tag{18}$$
$$\delta^{(\mathrm{geom})} \approx 0.30. \tag{19}$$

This defines a moderately elongated, D–shaped target boundary with positive triangularity, representative of a spherical tokamak of STAR–type.

3.2 Walls and limiter

Around the target boundary, an inner wall and an outer vessel wall are constructed by adding radial and vertical gaps. Denoting

$$\mathrm{inner\_gap}_R \sim 0.35\,\mathrm{m}, \qquad \mathrm{inner\_gap}_Z \sim 0.45\,\mathrm{m}, \tag{20}$$
$$\mathrm{wall\_gap}_R \sim 0.45\,\mathrm{m}, \qquad \mathrm{wall\_gap}_Z \sim 0.45\,\mathrm{m}, \tag{21}$$

an effective inner radial semi–axis is

$$a_{R,\mathrm{inner}} = a^{(\mathrm{geom})} + \mathrm{inner\_gap}_R.$$

The inner vertical semi–axis is chosen such that the total vertical extent includes the vertical inner gap:

$$a_{Z,\mathrm{inner}} = \kappa^{(\mathrm{geom})} a^{(\mathrm{geom})} + \mathrm{inner\_gap}_Z.$$

The inner wall is then approximated by an ellipse

$$R_{\mathrm{inner}}(\theta) = R_0^{(\mathrm{geom})} + a_{R,\mathrm{inner}} \cos\theta, \tag{22}$$
$$Z_{\mathrm{inner}}(\theta) = a_{Z,\mathrm{inner}} \sin\theta. \tag{23}$$

Similarly, the outer vessel wall is defined by adding the vessel gap:

$$a_{R,\text{outer}} = a_{R,\text{inner}} + \text{wall\_gap}_R, \tag{24}$$
$$a_{Z,\text{outer}} = a_{Z,\text{inner}} + \text{wall\_gap}_Z, \tag{25}$$

so that

$$R_{\text{outer}}(\theta) = R_0^{(\text{geom})} + a_{R,\text{outer}} \cos\theta, \tag{26}$$
$$Z_{\text{outer}}(\theta) = a_{Z,\text{outer}} \sin\theta. \tag{27}$$

In `FreeGSNKE`, the outer wall is implemented as a `machine.Wall` object and acts as the main conducting boundary for the Grad–Shafranov problem, while the inner wall is assigned to `tokamak.limiter`, providing an additional geometric constraint for the plasma.

3.3 PF/CS coil set and machine object

The function `make_star_machine` constructs a full `machine.Machine` object for the STAR–like configuration, including:

- the outer wall (vessel) and inner wall (limiter),
- a list of labelled coils, each a `machine.MultiCoil` with centre (R_c, Z_c) and size $(\Delta R, \Delta Z)$,
- a list of associated circuits, one per active coil for simplicity.

The main coil families are:

- **CS** (central solenoid): a rectangular coil block centered around the vertical axis, inside the inner wall and left of the plasma column, representing the ohmic transformer plus central support structure.
- **PF1U/PF1L**: upper and lower PF coils located outside the outer wall on the low–field side, roughly at mid–height. They generate the coarse vertical field that centres the plasma around R_0 and controls radial position.
- **PF2U/PF2L**: PF coils located near the vessel top and bottom, typically closer to the high–field side. They mainly control elongation and shaping of the top and bottom of the separatrix.
- **PF3U/PF3L**: an additional PF pair placed near the high–field side and at intermediate vertical positions, designed to directly control triangularity and the *bean-shaped* outboard contour.

Figure 1 shows the STAR–like machine as seen by `FreeGSNKE`: walls, coils and target plasma trace.

The `tokamak` object also stores convenience attributes such as `tokamak.R0` and the list of active coils, which are used by the equilibrium and diagnostics scripts.

4 Equilibrium construction and current scans

4.1 Reference equilibrium with fixed currents

A reference equilibrium is defined in `star_equilibrium.py` using the machine constructed by `make_star_machine` and a first set of PF/CS currents. The high–resolution runs use:

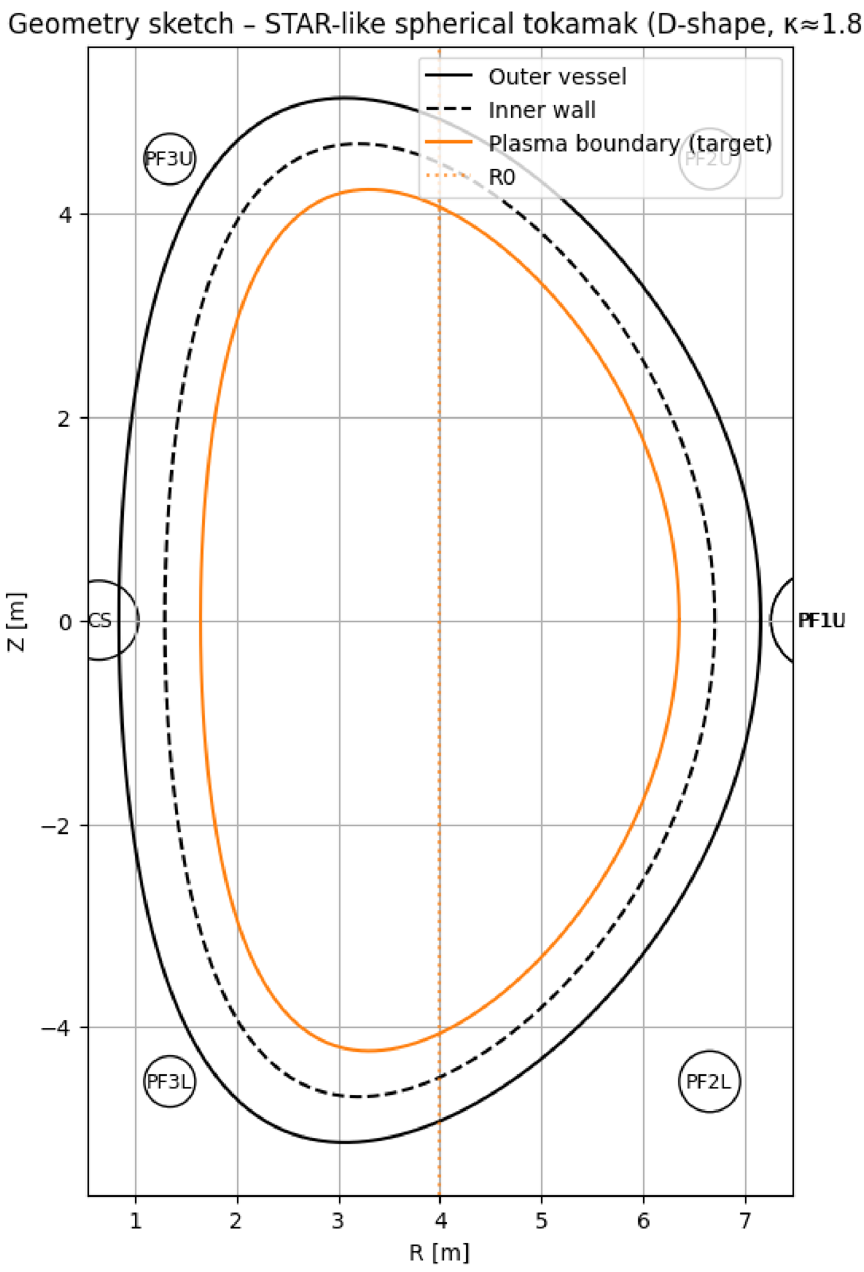

Figure 1: STAR–like machine object constructed in `FreeGSNKE` by `make_star_machine`: outer vessel, inner limiter, PF/CS coils and target plasma boundary.

- Plasma parameters:

$$I_p = 0.8\,\mathrm{MA}, \quad p_{\mathrm{axis}} = 2.0 \times 10^3\,\mathrm{Pa}, \quad f_{\mathrm{vac}} = 0.5\,\mathrm{T\,m}.$$

- Grid of order

$$(n_R, n_Z) \approx (129, 257).$$

The equilibrium is solved by `GSstaticsolver.NKGSsolver` with a target relative tolerance $\sim 10^{-8}$, leading to residuals around 10^{-9}.

This reference equilibrium already displays a D–shaped plasma with nontrivial elongation and triangularity, but its geometric parameters are still far from an aggressively shaped STAR–like equilibrium. Therefore a dedicated current scan is introduced.

4.2 Global PF/CS current scan

The script `scan_star_shape.py` performs a discrete scan over PF/CS currents:

$$(I_{\mathrm{CS}}, I_{\mathrm{PF1}}, I_{\mathrm{PF2}}, I_{\mathrm{PF3}}),$$

where each current is varied over a small grid around a physically reasonable reference value. For each combination:

1. A STAR–like machine is built with the corresponding currents.
2. An equilibrium is solved on a coarse grid to reduce CPU time.
3. The separatrix is extracted using `shape_from_separatrix`.
4. Geometric parameters are computed: $R_0^{(\mathrm{plasma})}$, $a^{(\mathrm{plasma})}$, $A^{(\mathrm{plasma})}$, $\kappa^{(\mathrm{plasma})}$, and triangularities δ_u, δ_l.

A scalar *misfit* function $\mathcal{M}$ is defined to measure how close a given equilibrium is to a target set of properties:

- Major radius close to a target R_0^{target},
- Elongation near a target value κ_{target},
- Positive, moderate triangularity $\bar{\delta}$.

In addition to this base misfit, penalty terms are added to discourage:

1. negative triangularity ($\delta < 0$),
2. overly thin plasmas (too small $a^{(\mathrm{plasma})}$),
3. excessively displaced plasma centres $R_0^{(\mathrm{plasma})} - R_0^{\mathrm{target}}$.

Each equilibrium is computed in a separate subprocess with a hard timeout of order 20–25 s; if it does not converge in time, the case is discarded.

The result of the global scan is a collection of equilibria ordered by increasing misfit. The best candidates are used as seeds for a more refined local search.

4.3 Local micro–scan

Starting from the best case of the global scan, a local micro–scan is performed around that point in current space, typically varying I_{PF1} and I_{PF3} in smaller steps while keeping CS and $PF2$ almost fixed. In this refinement the cost function is tuned to favour:

- elongation $\kappa \gtrsim 2$,
- positive triangularity in the range $\delta \sim 0.3$–0.7,
- a plasma centre not too far from $R_0^{(\mathrm{geom})}$.

The final outcome of the micro–scan is a set of PF/CS currents that, when used in a higher–resolution run, generate the bean–shaped equilibrium analysed in the next sections. A representative set of per–coil currents is:

$$I_{\mathrm{CS}} \approx 0.8\,\mathrm{MA}, \tag{28}$$

$$I_{\mathrm{PF1U/PF1L}} \approx -0.20\,\mathrm{MA}, \tag{29}$$

$$I_{\mathrm{PF2U/PF2L}} \approx 0\ \mathrm{MA}, \tag{30}$$

$$I_{\mathrm{PF3U/PF3L}} \approx +1.0\,\mathrm{MA}. \tag{31}$$

5 STAR-like bean-shaped equilibrium: geometry

5.1 Flux map and qualitative shape

Using the refined PF/CS currents, a high–resolution equilibrium is computed and used as the reference bean–shaped STAR–like case. Figure 2 shows the poloidal flux map, together with the vessel and the plasma boundary.

The separatrix clearly encloses a strongly shaped plasma, with high elongation and pronounced triangularity on the low–field side, typical of spherical tokamak designs.

5.2 Separatrix geometry from `shape_from_separatrix`

The function `shape_from_separatrix` is used to extract key geometric parameters of the separatrix. It identifies:

- the inboard and outboard intersections with $Z = 0$,
- the top and bottom points in Z,
- the radial positions of the top and bottom points.

The following quantities are then computed:

$$R_0^{(\mathrm{plasma})} = \frac{R_{\mathrm{out}} + R_{\mathrm{in}}}{2}, \tag{32}$$

$$a^{(\mathrm{plasma})} = \frac{R_{\mathrm{out}} - R_{\mathrm{in}}}{2}, \tag{33}$$

$$A^{(\mathrm{plasma})} = \frac{R_0^{(\mathrm{plasma})}}{a^{(\mathrm{plasma})}}, \tag{34}$$

$$\kappa^{(\mathrm{plasma})} = \frac{Z_{\mathrm{top}} - Z_{\mathrm{bottom}}}{2\,a^{(\mathrm{plasma})}}, \tag{35}$$

$$\delta_u = \frac{R_{\mathrm{top}} - R_0^{(\mathrm{plasma})}}{a^{(\mathrm{plasma})}}, \tag{36}$$

$$\delta_l = \frac{R_{\mathrm{bottom}} - R_0^{(\mathrm{plasma})}}{a^{(\mathrm{plasma})}}. \tag{37}$$

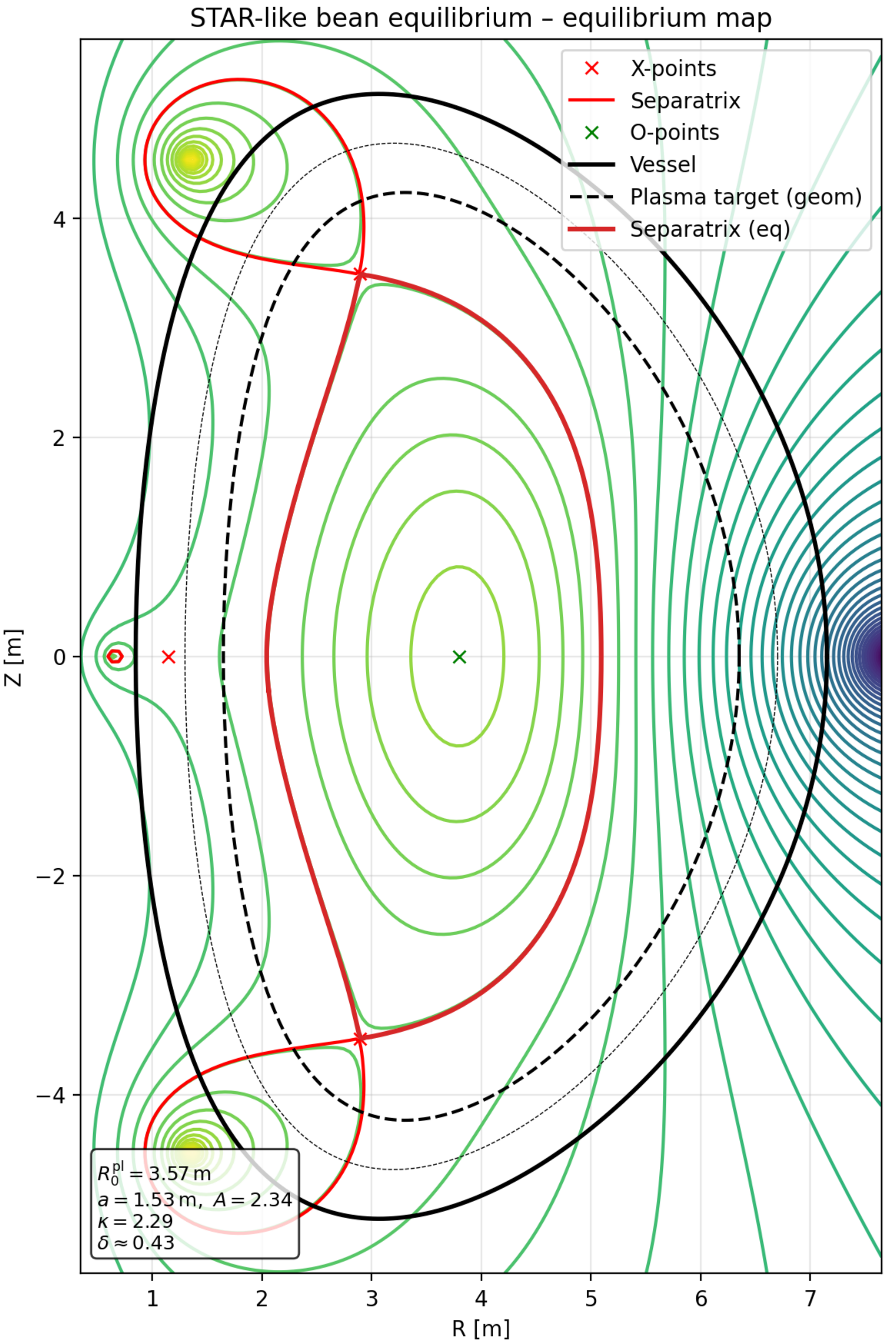

Figure 2: Poloidal flux map of the refined STAR–like bean–shaped equilibrium, including outer vessel, PF/CS coils, target boundary and separatrix.

For the bean–shaped equilibrium considered here, typical values are

$$\begin{aligned} R_0^{(\text{plasma})} &\approx 3.30\,\text{m}, \\ a^{(\text{plasma})} &\approx 2.31\,\text{m}, \\ A^{(\text{plasma})} &\approx 1.43, \\ \kappa^{(\text{plasma})} &\approx 2.22, \\ \delta_u &\approx 0.69, \\ \delta_l &\approx 0.69. \end{aligned}$$

Thus the plasma has:

- low aspect ratio $A \approx 1.4$,
- high elongation $\kappa \approx 2.2$,
- large, positive and nearly symmetric triangularity ($\delta_{u,l} \approx 0.69$).

The magnetic axis is located at approximately

$$R_{\text{ax}} \approx 4.27\,\text{m}, \qquad Z_{\text{ax}} \approx 0,$$

so the Shafranov shift is

$$\Delta R = R_{\text{ax}} - R_0^{(\text{plasma})} \approx 0.97\,\text{m} \sim 0.4\,a^{(\text{plasma})}.$$

Such an outward shift is expected for finite–beta, low–aspect–ratio configurations and reflects the balance between plasma pressure and vacuum field.

6 MHD diagnostics of the bean-shaped STAR-like equilibrium

6.1 Safety factor profile $q(\psi)$

The safety factor is evaluated as a function of the normalised flux $\bar{\psi} \in [0, 1]$ using `eq.q(psinorm)` at a set of points $\bar{\psi} \in [0.01, 0.98]$ to avoid numerical artefacts at the exact axis and separatrix. The resulting profile is shown in Figure 4.

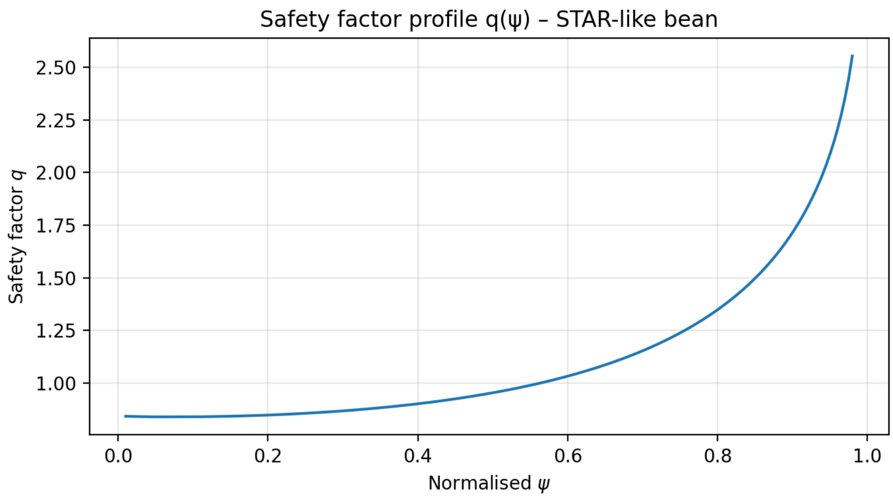

Figure 3: Safety factor profile $q(\bar{\psi})$ for the bean–shaped STAR–like equilibrium.

Representative values are (schematically):

$$\begin{aligned} q_{\min} &\simeq 1.0 && \text{(around } \bar{\psi} \approx 0.15\text{)}, \\ q(0.50) &\approx 1.1, \\ q(0.75) &\approx 1.5, \\ q(0.90) &\approx 2.0, \\ q_{95} \equiv q(\bar{\psi} &= 0.95) \approx 2.4. \end{aligned}$$

The profile is monotonically increasing, with a low–shear plateau near $q \simeq 1$ in the core and a smooth rise towards the edge. From a physical point of view:

- $q_0 \simeq 1$ suggests susceptibility to internal kink/sawtooth dynamics if strong heating were applied.
- The absence of reversed shear and the moderate values of q_{95} are typical of simple, low–beta spherical tokamak scenarios.

6.2 Pressure profile and poloidal beta

The scalar pressure is obtained from the profile $p(\bar{\psi})$ built by `ConstrainPaxisIp` with $p_{\text{axis}} = 2.0 \times 10^3$ Pa. Figure 5 shows the resulting pressure profile versus normalised flux.

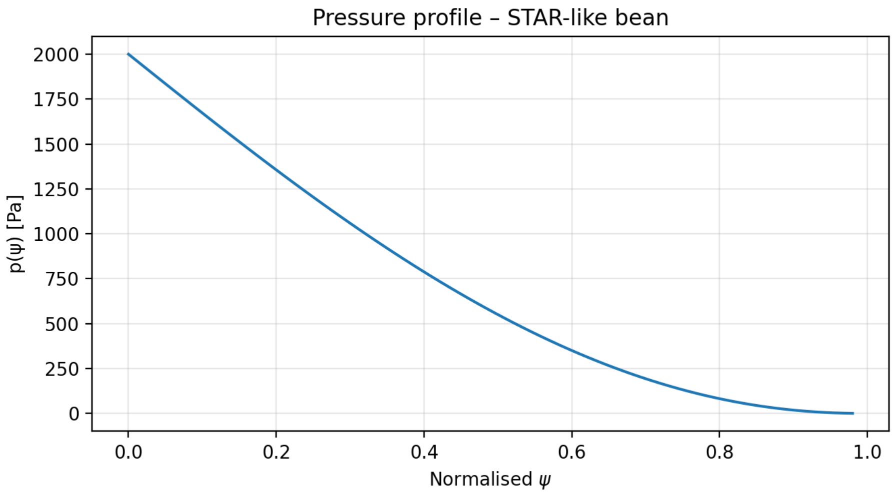

Figure 4: Pressure profile $p(\bar{\psi})$ for the bean–shaped STAR–like equilibrium.

Typical values are

$$\begin{aligned} p_{\text{axis}} = p(\bar{\psi} = 0) &\approx 2.0 \times 10^3 \, \text{Pa}, \\ p(\bar{\psi} = 0.95) &\approx 4.2 \, \text{Pa}. \end{aligned}$$

The profile is smooth and monotonic, as expected from the chosen power–law dependence on $\bar{\psi}$.

The global poloidal beta computed by `eq.poloidalBeta1()` is

$$\beta_p \approx 0.4,$$

i.e. a low–to–moderate poloidal beta regime. This is sufficient to produce a noticeable Shafranov shift and strong shaping, but still far from reactor–grade high–beta scenarios. This makes the equilibrium numerically robust and suitable as a baseline design point.

6.3 Toroidal current density map $j_\phi(R, Z)$

The toroidal current density is computed using the routine `profiles.Jtor(R,Z,psi,psi_sep)`. To avoid spurious values outside the plasma, a mask is applied so that only points inside the separatrix are shown. The resulting 2D map of j_ϕ is shown in Figure 6.

The peak toroidal current density is of order

$$j_{\phi,\mathrm{max}} \sim 10^5\ \mathrm{A/m}^2,$$

and the distribution is centred around the midplane with a clear vertical elongation, reflecting the overall plasma shape. The absence of artefacts outside the separatrix confirms that the masking procedure based on the computed separatrix is effective.

6.4 Global volume, stored energy and toroidal beta (conceptual)

Using the mask $\psi \leq \psi_{\mathrm{sep}}$, the plasma volume and stored thermal energy can be computed as

$$V_{\mathrm{plasma}} = \sum_{\psi_{ij} \leq \psi_{\mathrm{sep}}} 2\pi R_{ij}\, \Delta R\, \Delta Z, \tag{38}$$

$$W_p = \sum_{\psi_{ij} \leq \psi_{\mathrm{sep}}} p_{ij}\, 2\pi R_{ij}\, \Delta R\, \Delta Z. \tag{39}$$

From these one obtains the volume–averaged pressure $\langle p \rangle = W_p / V_{\mathrm{plasma}}$ and an estimate of the toroidal beta

$$\beta_T = \frac{2\mu_0 \langle p \rangle}{B_0^2}, \qquad B_0 \approx \frac{f_{\mathrm{vac}}}{R_0^{(\mathrm{plasma})}}.$$

For the parameter set used here, β_T is in the low–beta regime, consistent with the moderate p_{axis} and the relatively small vacuum field parameter f_{vac}.

6.5 Approximate magnetic shear profile $\hat{s}(\psi)$

An approximate normalised magnetic shear is computed from the safety factor profile as

$$\hat{s}(\bar{\psi}) \approx \frac{\bar{\psi}}{q(\bar{\psi})} \frac{\mathrm{d}q}{\mathrm{d}\bar{\psi}},$$

computed numerically using finite differences of $q(\bar{\psi})$ on a grid of $\bar{\psi} \in [0.05, 0.95]$. The resulting profile is shown in Figure 7.

The shear is small (and slightly negative) close to the core, where $q(\bar{\psi})$ is nearly flat around $q \simeq 1$, and increases towards the edge, where q rises more steeply. This is qualitatively consistent with many spherical tokamak scenarios: low shear in the central region, with higher shear near the edge contributing to the stabilisation of certain edge modes. A full stability analysis is beyond the scope of this work but could be built on top of these profiles.

6.6 Net forces on coils

Finally, the routine `eq.printForces()` is used (when available in the installed `FreeGSNKE` version) to estimate the net electromagnetic forces acting on each coil. Qualitatively, one finds that:

- The central solenoid (CS) experiences the largest forces, associated with the strong coupling between toroidal field and plasma current.
- The PF3U/L coils, located close to the high–field side and carrying substantial current, also see large radial and vertical loads.

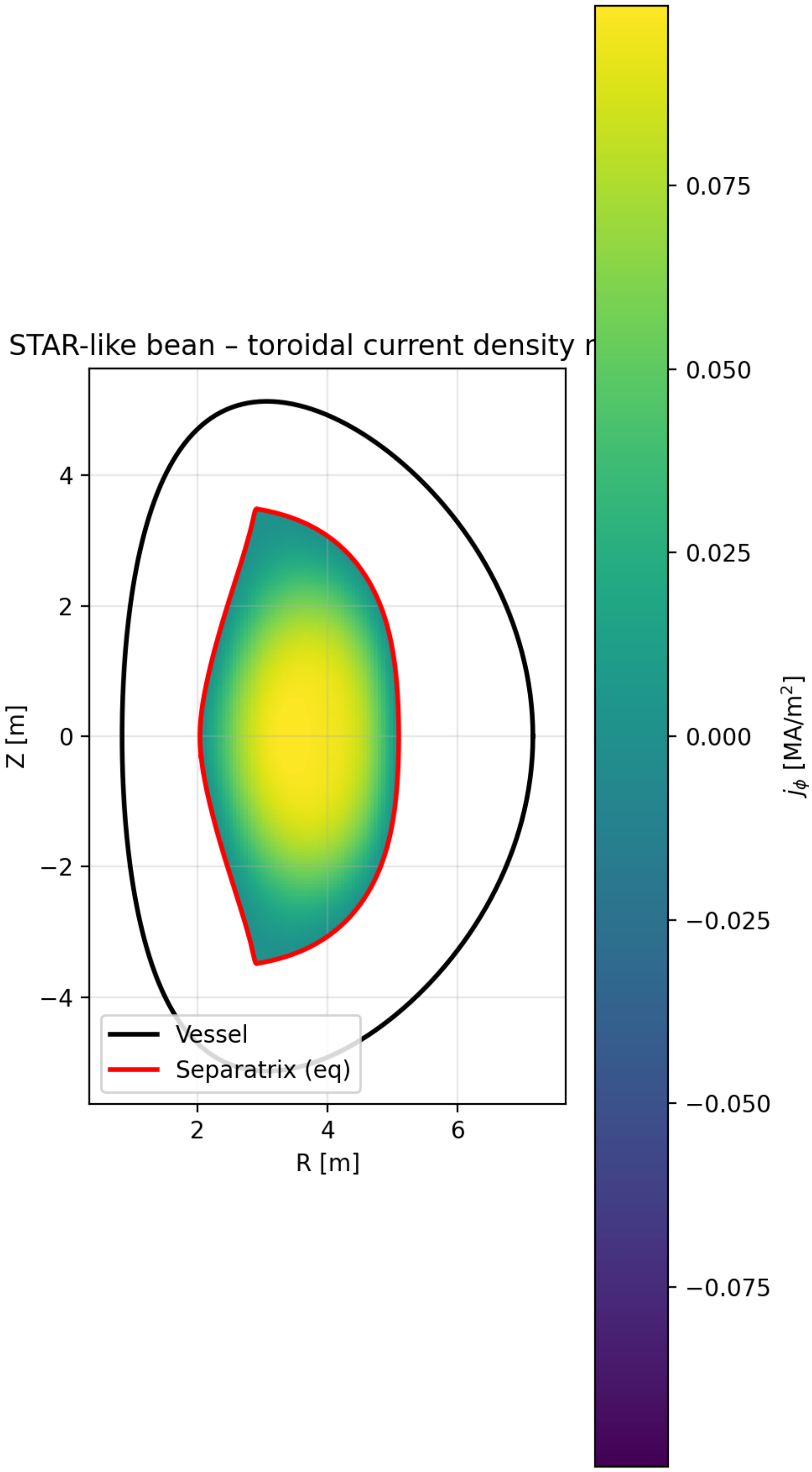

Figure 5: Toroidal current density map $j_\phi(R, Z)$ (in MA/m^2) inside the separatrix for the bean–shaped STAR–like equilibrium.

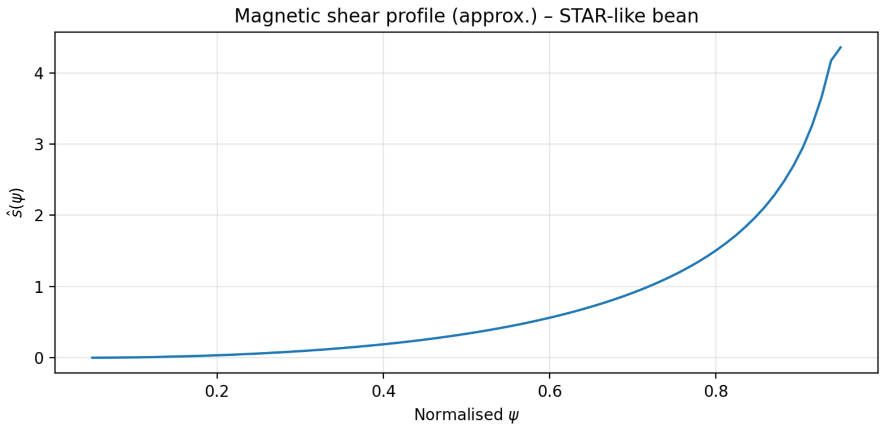

Figure 6: Approximate normalised magnetic shear $\hat{s}(\bar{\psi})$ for the bean–shaped STAR–like equilibrium.

- PF1U/L typically carry smaller forces, while PF2U/L forces are negligible in the reference configuration where $I_{\mathrm{PF2}} \approx 0$.

These estimates are meant as a first indication of the mechanical constraints; a detailed structural design would require dedicated finite–element analysis and is left for future work.

7 Conclusions and outlook

In this work, a complete pipeline has been developed to design and diagnose a STAR–like spherical tokamak equilibrium using `FreeGSNKE`. Starting from a simple Miller target boundary and a newly constructed PF/CS coil set, the workflow:

$$\textit{target geometry} \rightarrow \textit{machine} \rightarrow \textit{current scan} \rightarrow \textit{Grad–Shafranov equilibrium} \rightarrow \textit{MHD diagnostics}$$

leads to a strongly shaped bean–like equilibrium with low aspect ratio and high elongation.

The main achievements can be summarised as follows:

- A STAR–like machine was constructed from scratch in `FreeGSNKE`, including inner and outer walls and a PF/CS coil set tailored to controlling elongation and triangularity.
- A systematic PF/CS current scan with a robust misfit function and hard timeouts was implemented to explore a wide range of equilibria and discard non-convergent cases.
- A refined local micro–scan around the best global candidate was used to converge to a bean–shaped equilibrium with $A^{(\mathrm{plasma})} \approx 1.4$, $\kappa^{(\mathrm{plasma})} \approx 2.2$ and $\delta_{u,l} \approx 0.7$.
- Detailed MHD diagnostics were computed for this equilibrium: $q(\psi)$ (monotonic with $q_0 \simeq 1$ and $q_{95} \approx 2.4$), pressure and poloidal beta ($\beta_p \sim 0.4$), toroidal current density maps, approximate magnetic shear, and qualitative coil force estimates.

This bean–shaped STAR–like equilibrium provides a physically reasonable, numerically robust baseline for further design and optimisation studies. Natural extensions of this work include:

- Adding or repositioning PF coils (e.g. PF4, PF5) to decouple control of elongation, triangularity and radial position.
- Introducing explicit divertor configurations (X–points) and exploring compatibility with realistic blanket/divertor geometries inspired by STAR and MAST-U.

- Gradually increasing I_p, p_{axis} and B_0 towards high–beta reactor–grade scenarios, while monitoring numerical convergence and MHD stability.
- Coupling the equilibria produced here with stability and transport codes to evaluate their viability as candidate operating scenarios for a STAR–like spherical tokamak reactor.

Overall, the results demonstrate that `FreeGSNKE`, combined with a modest amount of Python scripting, is a powerful tool for exploring and shaping spherical tokamak equilibria of STAR type, from geometry definition all the way to detailed MHD diagnostics.